Available online at www.sciencedirect.com
SCIENCE DIRECT®
PERGAMON
Polyhedron 22 (2003) 3115–3122
POLYHEDRON
www.elsevier.com/locate/poly

Synthesis, crystal structure and magnetic properties of $[Cr_2Cu_2(bpy)_4(ox)_5]\cdot 2H_2O$. An oxalato-bridged heterometallic tetramer

Eugenio Coronado *, Mari Carmen Giménez, Carlos J. Gómez-García, Francisco M. Romero *

Institut de Ciència Molecular, Universitat de València, Dr. Moliner 50, Burjassot 46100, Spain

Received 15 April 2003; accepted 1 July 2003

Abstract

A new heterometallic tetramer of formula $[Cr_2Cu_2(bpy)_4(ox)_5]\cdot 2H_2O$ (**1**) (bpy = 2,2′-bipyridine; ox = oxalate dianion) has been prepared and characterised by single-crystal X-ray diffraction, magnetic susceptibility measurements and ESR spectroscopy. The tetranuclear unit in **1** can be viewed as the combination of two terminal $[Cr(bpy)_2(ox)]^-$ units with a central oxalato-bridged copper(II) dimer. The chromium ions are in a distorted octahedral environment with metal–ligand distances ranging from 1.944(4) to 2.064(5) Å. The copper(II) centres lie in an axially distorted octahedron. The axial positions are occupied by one oxygen atom belonging to the central bridging oxalate anion [O(9)–Cu(1): 2.245(5) Å] and one oxygen atom coming from the $[Cr(bpy)_2(ox)]^-$ moiety [O(7)–Cu(1): 2.357(5) Å]. The N_2O_2 equatorial environment is formed by a bpy ligand [Cu–N mean distance: 1.989(6) Å] and the remaining oxygen atoms [Cu–O mean distance: 2.162(5) Å]. The magnetic properties of **1** have been investigated in the 2–300 K temperature range. A ferromagnetic interaction between the copper(II) centres ($J_1 = +2$ cm^{-1}) is observed, whereas the interaction between the adjacent chromium(III) and copper(II) cations is weakly antiferromagnetic ($J_2 = -0.65$ cm^{-1}).

Keywords: Synthesis; Crystal structures; Magnetic properties; Oxalato complexes

1. Introduction

Homoleptic oxalato complexes, $[M^{III}(ox)_3]^{3-}$ (ox = oxalate dianion), have proved to be useful precursors for the synthesis of anionic two- (2D) and three-dimensional (3D) magnetic lattices [1–3]. The dimensionality of these systems is directly related to the presence of a given countercation, A^+, which can be viewed as a templating agent of the overall structure [4]. Quaternary onium cations [5,6] give rise to 2D structures of the type $A[M^{II}M^{III}(ox)_3]$, while tris-chelated $[Z(bpy)_3]^{2+}$ (bpy = 2,2′-bipyridine) species induce the formation of chiral structures [7,8] of formulae $[M^{II}_2(ox)_3]^-$, $[M^{I}M^{III}(ox)_3]^-$ and $[M^{II}M^{III}(ox)_3]^-$. 2D structures offer the possibility to combine in the same compound alternating layers that give rise to two different collective properties. For instance, replacing the quaternary onium cations by organic donors of the TTF family affords materials showing electrical conductivity and ferromagnetism [9]. 3D structures are more suitable for the combination of ferromagnetism with a molecular property, like luminescence [10]. In this context, the family of compounds $[Ru(bpy)_3][M^{II}M^{III}(ox)_3](ClO_4)$ has been studied, although its photophysical properties have not yet been addressed in detail [11].

Recently, attention has also been paid to the use of heteroleptic oxalato complexes of the type $[Cr(L)(ox)_2]^-$ (L = α-diimine) in the synthesis of heterometallic compounds [12–14]. As expected, the combination of the $[Cr(bpy)(ox)_2]^-$ building block [15] with divalent metal ions affords the series $[M^{II}Cr_2(bpy)_2(ox)_4(H_2O)_x]$ with 1:2 M(II):Cr(III) stoichiometry [16–18]. We have been interested in these compounds as starting materials for

* Corresponding authors.
E-mail address: fmrm@uv.es (F.M. Romero).

0277-5387/$ - see front matter © 2003 Elsevier Ltd. All rights reserved.
doi:10.1016/S0277-5387(03)00462-5

the preparation of spinels with potential applications in the field of ceramic pigments. However, a systematic study of the reaction conditions (stoichiometry, concentration,...) permitted us to isolate the new tetranuclear complex $[Cr_2Cu_2(bpy)_4(ox)_5]\cdot 2H_2O$ (**1**). We report herein the crystal structure and the magnetic properties of this novel Cr_2Cu_2 tetramer.

2. Experimental

2.1. Materials

Chromium(III) chloride hexahydrate, 2-2′-bipyridine, sodium oxalate, barium(II) chloride dihydrate and copper(II) sulfate pentahydrate were purchased from Fluka and all the manipulations were performed using materials as received.

2.2. Preparation of $Ba[Cr(bpy)_2(ox)]_2\cdot 3H_2O$ precursor [15]

An aqueous suspension (100 ml) containing stoichiometric amounts of $CrCl_3\cdot 6H_2O$ (53 mg, 2 mmol), 2,2′-bipyridine (32 mg, 2 mmol) and sodium oxalate (53 mg, 4 mmol) was refluxed (100 °C) during half-an-hour under continuous stirring. The initially green solution turned red-violet upon warming. After a few minutes, a light-pink microcrystalline powder of $[Cr(bpy)(ox)_2]$ $[Cr(bpy)_2(ox)]$ precipitates. The solid was immediately filtered off. $BaCl_2\cdot 6H_2O$ (24 mg, 1 mmol), dissolved in a minimum amount of water (approximately 2.5 ml), was added dropwise to the filtrate, under stirring at room temperature. The resulting mixture was stirred for 1 h to promote complete precipitation of a dark pink powder of $Ba[Cr(bpy)_2(ox)]_2\cdot 3H_2O$, which was removed by filtration and washed with water. Red single crystals of $Ba[Cr(bpy)_2(ox)]_2\cdot 3H_2O$ were obtained by slow evaporation from the filtrate. (306 mg, 35%) $\bar{\nu}_{max}/cm^{-1}$: 3468m, 3075w, 2923w, 1718vs, 1687vs, 1655vs, 1498m, 1475s, 1447w, 1389m, 1320w, 1252w, 1162w, 1106w, 1063w, 1036w, 1023w, 897w, 809w, 769m, 730m, 654w, 548w, 476m, 450w; (metal analysis (%): Ba, 34.3; Cr, 65.7).

2.3. Preparation of $[Cr_2Cu_2(bpy)_4(ox)_5]\cdot 2H_2O$

A suspension of $Ba[Cr(bpy)_2(ox)]_2\cdot 3H_2O$ (26 mg, 0.25 mmol) in 25 ml of water was allowed to react with $CuSO_4\cdot 5H_2O$ (12 mg, 0.50 mmol) dissolved in 10 ml of water. The resulting mixture was stirred for 3 h to promote complete precipitation of barium sulfate, which was removed by filtration. After a few days, large brown crystals were formed together with a light-blue precipitate that analysed as copper(II) oxalate. (62 mg, 20%), (Found: C, 45.0; H, 2.7; N, 8.4. $C_{50}H_{36}Cr_2Cu_2N_8O_{22}$ requires C, 45.1; H, 2.7; N, 8.4%); $\bar{\nu}_{max}/cm^{-1}$: 3488s, 3117w, 3081w, 3030w, 2923w, 2853w, 1718vs, 1678vs, 1653vs, 1604s, 1498m, 1475m, 1448s, 1371w, 1315w, 1283w, 1237w, 1177w, 1160w, 1107w, 1061w, 1035w, 1023w, 980w, 893w, 807m, 779m, 731w, 667w, 652w, 552w, 481w; (Metal analysis (%): Cu, 49.4; Cr 50.6).

2.4. IR characterisation

The heterometallic tetramer of formula $[Cr_2Cu_2(bpy)_4(ox)_5]\cdot 2H_2O$ shows four intense IR bands between 1718 and 1653 cm^{-1} due to asymmetric ν_{CO} stretching vibrations of the oxalate anions. The high number of bands in this region suggests the existence of two types of oxalate groups in the crystal lattice (bridging and terminal). The bands between 1448–1315 and 807–779 cm^{-1} are attributed to ν_{CO} and ν_{CC} oxalate symmetric stretching vibrations, respectively. The lower wavenumber band (552–481 cm^{-1}) can be assigned to (–Cu–O–) and (–Cr–O–) deformation vibration. In the 3500 cm^{-1} region, a strong and broad absorption is observed, in agreement with the presence of uncoordinated water molecules of crystallisation in the complex. Other significant bands belong to the 2,2′-bipyridine ligand.

2.5. Physical techniques

Elemental analysis (C, H, N) and the measurement of Cr:Cu ratios were performed by the SCSIE of the University of Valencia on a CE INSTRUMENTS EA 1110 CHNS elemental analyser and a Philips ESEM X230 scanning electron microscope equipped with an EDAX DX-4 microsonde.

The infrared spectrum was recorded on a Nicolet 800 FTIR spectrophotometer as KBr pellets from 4000 to 400 cm^{-1}.

Magnetic susceptibility measurements of a polycrystalline sample were carried out using a magnetometer (Quantum Design MPMS-XL-5) equipped with a SQUID sensor. The dc measurements were performed in the temperature range 2–300 K at a magnetic field of 0.1 T (1000 Oe). The magnetisation was performed between 0 and 5 T at 2 K.

ESR measurements were performed on a grinded polycrystalline sample at X-band in the T range 300–4.2 K with a BRUKER ELEXSYS E-500 spectrometer equipped with a He-cryostat.

2.6. X-ray data collection and structure determination

Good-quality single crystals of $[Cr_2Cu_2(bpy)_4(ox)_5]\cdot 2H_2O$ were collected and one of them of dimensions $0.31\times 0.17\times 0.16$ mm was mounted on a CAD4 Enraf-Nonius X-ray diffractometer. Unit cell parameters and orientation matrix were determined by least-

squares fit of 25 independent reflections. Data collection was performed with the ω-scan technique with three standard reflections measured every 2 h which showed no significant decay. Lorentz, polarisation, and empiric absorption (Ψ scan) corrections were carried out. The structure was solved by direct methods using the SIR 97 program [19] and was refined on F^2 using the SHELXL-97 program [20].

In the structural determination the heavy atoms were found immediately and the other atoms were located through successive Fourier differences. All non-hydrogen atoms were refined anisotropically. One of the water molecules O(12) was disordered in two alternative positions, O(12A) and O(12B) with occupancy factors of 0.25 and 0.75, respectively. The hydrogen atoms of the water molecules were calculated on the basis of geometry and force-field considerations [21]. The hydrogen atoms of the 2,2′-bipyridine ligands were set in calculated positions and refined as riding atoms with a common fixed isotropic thermal parameter. Crystallographic data and refinement parameters are summarised in Table 1. Table 2 gathers selected bond lengths and angles.

3. Results and discussion

3.1. Crystal structure

The structure of compound **1** consists of neutral tetranuclear complexes (Fig. 1) and water molecules of crystallisation. Each tetranuclear complex is built from two $[Cr(bpy)(ox)_2]^-$ subunits acting as bidentate ligands towards a central μ-oxalatobis[(2,2′-bipyridine)copper(II)] fragment. An inversion centre is located in the middle of the C—C bond of this central μ-oxalato bridge and the structure of the complex is centrosymmetric.

Table 1
Crystal data and structure refinement data for **1**

Formula	$C_{25}H_{18}CrCuN_4O_{11}$
FW	665.98
Crystal system	triclinic
Space group	$P\bar{1}$
a (Å)	9.6740(14)
b (Å)	10.9636(17)
c (Å)	14.543(5)
α (°)	100.076(3)
β (°)	94.492(4)
γ (°)	114.861(3)
V (Å)	1357.9(5)
Z	2
T (K)	293
λ (Å)	0.71073
ρ_{calc} (g cm^3)	1.673
R_1[a]	0.0787
R_2[b]	0.1792

[a] $R_1 = \sum(F_o - F_c)/\sum(F_o)$.
[b] $R_2 = [\sum[\omega(F_o^2 - F_c^2)^2]/\sum[\omega(F_o^2)^2]]^{1/2}$; $\omega = 1/[\sum_2(F_o^2) + (0.1446P)^2 + 4.8035P]$, where $P = (F_o^2 + 2F_c^2)/3$.

Table 2
Selected bond lengths (Å) and angles (°) for **1**

Chromium environment	
Bond lengths	
Cr(1)–N(1)	2.064(5)
Cr(1)–N(2)	2.044(5)
Cr(1)–O(1)	1.944(4)
Cr(1)–O(2)	1.946(4)
Cr(1)–O(5)	1.977(4)
Cr(1)–O(6)	2.004(4)
Bond angles	
O(1)–Cr(1)–O(2)	83.63(19)
O(1)–Cr(1)–O(5)	92.4(2)
O(2)–Cr(1)–O(5)	90.09(19)
O(1)–Cr(1)–O(6)	171.42(18)
O(2)–Cr(1)–O(6)	89.75(19)
O(5)–Cr(1)–O(6)	82.19(19)
O(1)–Cr(1)–N(2)	91.4(2)
O(2)–Cr(1)–N(2)	95.6(2)
O(5)–Cr(1)–N(2)	173.5(2)
O(6)–Cr(1)–N(2)	94.7(2)
O(1)–Cr(1)–N(1)	95.1(2)
O(2)–Cr(1)–N(1)	174.4(2)
O(5)–Cr(1)–N(1)	95.45(19)
O(6)–Cr(1)–N(1)	92.0 (2)
N(2)–Cr(1)–N(1)	78.9(2)
Copper environment	
Bond lengths	
Cu(1)–N(3)	2.001(6)
Cu(1)–N(4)	1.977(5)
Cu(1)–O(7)	2.357(5)
Cu(1)–O(8)	2.080(5)
Cu(1)–O(9)	2.245(5)
Cu(1)–O(10)	1.964(5)
Bond angles	
O(10)–Cu(1)–N(4)	175.8(2)
O(10)–Cu(1)–N(3)	94.8(2)
N(4)–Cu(1)–N(3)	81.4(2)
O(10)–Cu(1)–O(8)	88.1(2)
N(4)–Cu(1)–O(8)	95.9(2)
N(3)–Cu(1)–O(8)	174.3(2)
O(10)–Cu(1)–O(9)	79.65(18)
N(4)–Cu(1)–O(9)	99.3 (2)
N(3)–Cu(1)–O(9)	99.9(2)
O(8)–Cu(1)–O(9)	85.45(18)
O(10)–Cu(1)–O(7)	91.66(18)
N(4)–Cu(1)–O(7)	90.6(2)
N(3)–Cu(1)–O(7)	98.97(19)
O(8)–Cu(1)–O(7)	76.03(17)
O(9)–Cu(1)–O(7)	159.83(16)

This is in contrast with the situation found in a similar tetranuclear compound $\{[Cr(phen)(ox)_2]_2[Mn_2(bpy)_2(H_2O)_2(ox)]\} \cdot 6H_2O$, where two $[Cr(phen)(ox)_2]$ anions bind as unidentate ligands to a central μ-oxalatobis[(2,2′-bipyridine)manganese(II)] fragment, giving rise to a non-centrosymmetric structure [14].

The chromium atoms are located in a slightly distorted octahedral environment. The Cr—O bond distances for the terminal oxalato ligand (Cr(1)–O(1) = Cr(1)–O(2): 1.946(4) Å) are somewhat shorter than for the bridging ligand (Cr(1)–O(5): 1.977(4) and

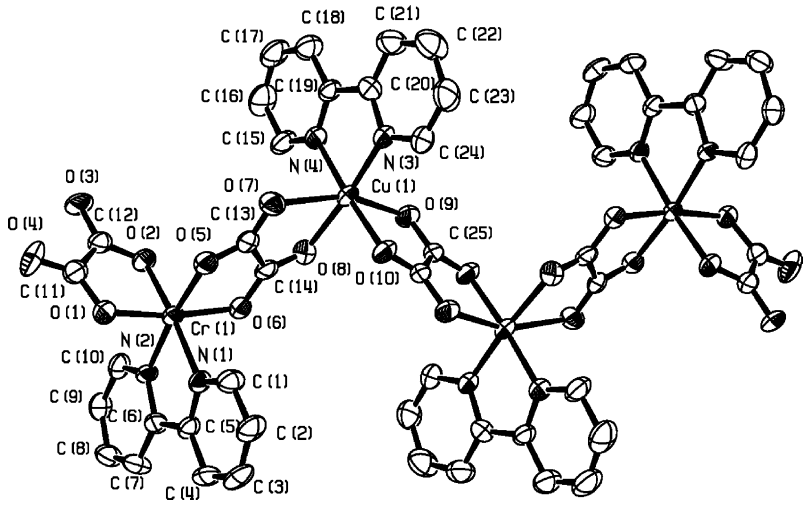

Fig. 1. ORTEP view of the $[Cr_2Cu_2(bpy)_4(ox)_5]$ tetranuclear unit of **1**. Thermal ellipsoids are plotted at the 50% probability level.

Cr(1)–O(6): 2.004(5) Å). The chelate angle N(1)–Cr(1)–N(2) (78.9(2)°) is smaller than the two oxalato chelate angles (O(1)–Cr(1)–O(2): 83.63(19)°; O(5)–Cr(1)–O(6): 82.19(19)°). These structural features are in agreement with other previously reported $[Cr(bpy)(ox)_2]^-$ units [14]. The copper atoms show the expected axially elongated octahedral coordination (Jahn–Teller effect). The resulting N_2O_4 environment is formed by two nitrogen atoms from a bpy ligand, N(3) and N(4), two oxygen atoms, O(7) and O(8), belonging to a $[Cr(bpy)(ox)_2]^-$ moiety, and two oxygen atoms, O(9) and O(10), from the central μ-oxalato bridging unit. As expected, the bipyridine ligand is found in the equatorial plane (Cu(1)–N(3): 2.001(6) Å; Cu(1)–N(4): 1.977(5) Å) with Cu–O distances (Cu(1)–O(8): 2.080(5) Å; Cu(1)–O(10): 1.964(5) Å) shorter than in the axial direction (Cu(1)–O(7): 2.357(5) Å; Cu(1)–O(9): 2.245(5) Å). The distance between copper(II) ions is Cu(1)–Cu(1)($-x, -y, -z$): 5.438(2) Å, while the chromium–copper separation Cr(1)–Cu(1) equals 5.4473(17) Å. The dihedral angles between the N_2O_2Cu basal plane and the mean planes of the bridging oxalate anions are 81.69(19)° (for the cen-

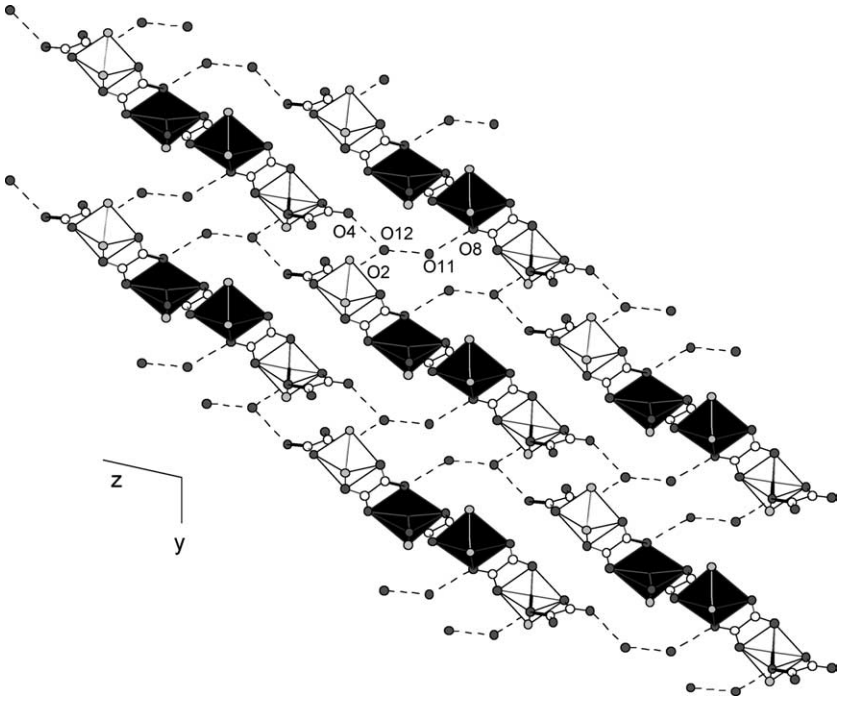

Fig. 2. Projection of the crystal structure of **1** onto the *bc*-plane showing the intricate hydrogen-bonded network. Plain octahedra denote metal environments (black: Cu; white: Cr). Dashed lines refer to hydrogen bonds. Bipyridine carbon atoms are omitted.

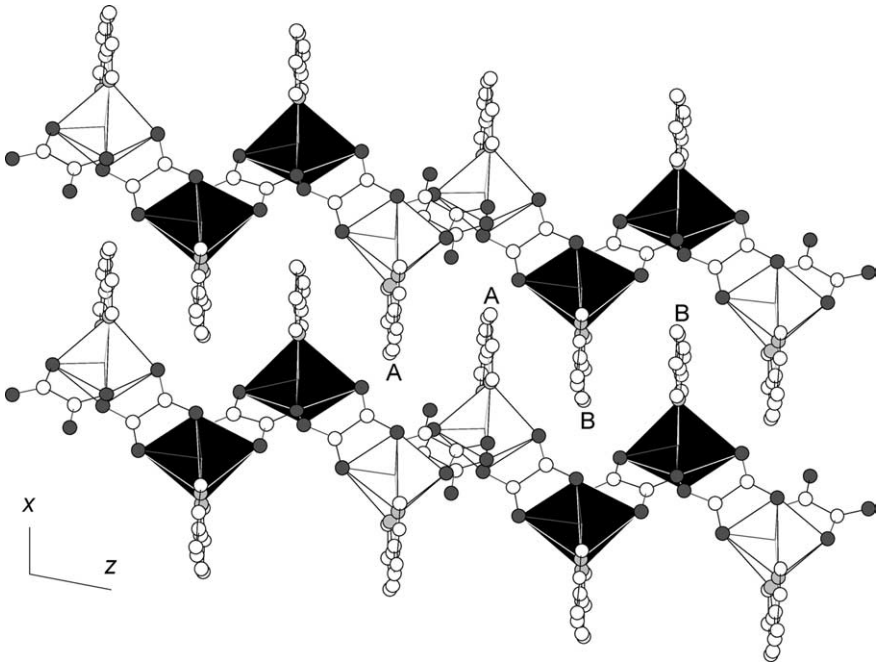

Fig. 3. Projection of the crystal structure of **1** onto the *ac*-plane showing the stacking of bpy ligands along the *z*-axis. Plain octahedra denote metal environments (black: Cu; white: Cr).

tral bridging unit) and 86.02(16)° (for the Cr–Cu bridge).

Two water molecules are present in the crystal structure of **1**. One molecule bridges via hydrogen bonds two terminal oxalate anions corresponding to adjacent Cr_2Cu_2 complexes (O(12B)–O(2): 2.982(13) Å; O(12B)–O(4)$(-x, -y-1, -z+1)$: 3.067(15) Å). This organises chains of tetramers running along the $[0\,\bar{1}\,1]$ direction (Fig. 2). The remaining water molecule is hydrogen-bonded to a bridging oxalate of a $[Cr(bpy)(ox)_2]^-$ unit (O(11)–O(8): 3.011(13) Å). Noteworthy is the presence of π–π interactions (Fig. 3) between bpy ligands from neighbouring chains of tetramers. This results in the formation of one-dimensional stacks with AABB topology. The bpy–bpy mean plane separations between coplanar molecules are 3.67(5) Å (AA dimer) and 3.68(4) Å (BB dimer). AA and BB dimers are slightly tilted (5.53(7)°), the closest distance between them being 3.497(11) Å.

3.2. Magnetic properties

The thermal variation of the $\chi_M T$ product (χ_M is the molar magnetic susceptibility, T is the absolute temperature) for compound **1** was measured in the 2–300 K temperature range (Fig. 4). At room temperature, the $\chi_M T$ value (4.46 emu K mol^{-1}) is close to the one expected for the sum of two $S_{Cu} = 1/2$ and two $S_{Cr} = 3/2$ isolated spins. This value remains constant on cooling the sample down to 20 K. Below this temperature, $\chi_M T$ decreases smoothly and equals 2.26 emu K mol^{-1} at 2.0 K. These data are characteristic of a global antiferromagnetic behaviour, although a significant effect of the axial zero-field splitting of the chromium ions cannot be discarded. Further, the absence of a maximum in the susceptibility curve is indicative of weak magnetic interactions. The magnetisation versus field curve increases continuously with increasing field in the [0–5] Tesla range. The magnetisation value at 5 T

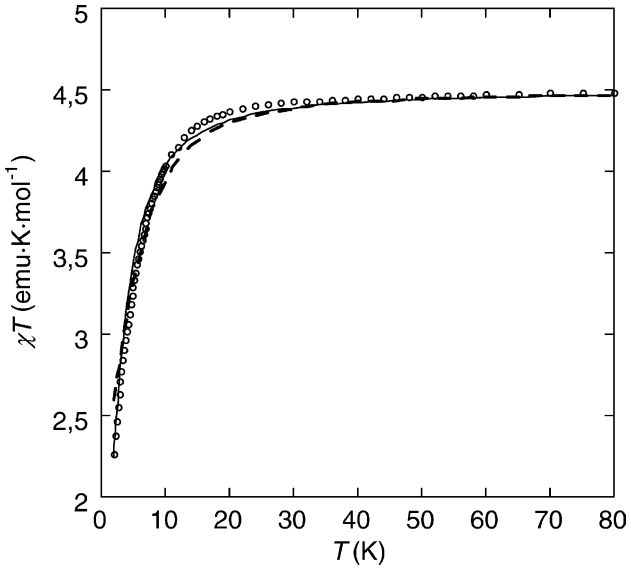

Fig. 4. Thermal variation of the $\chi_M T$ product of **1**. The continuous line represents the best-fit data to the linear tetrameric model described by Eq. (1). The dashed line refers to the best-fit data assuming $j = 0$.

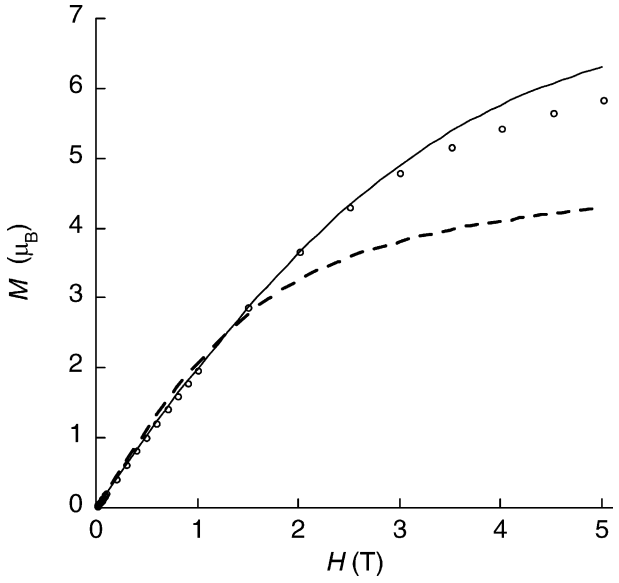

Fig. 5. Field dependence of the isothermal magnetisation of **1** at 2 K. The continuous line represents the best-fit data to the linear tetrameric model described by Eq. (1). The dashed line refers to the best-fit data assuming $j = 0$.

($M = 5.8\ \mu_B$) indicates that saturation is not reached at the higher field of the experiment (Fig. 5). Taking into account the crystal structure of **1** (Cr–Cu–Cu–Cr centrosymmetric linear tetramer), the analysis of the magnetic data can be performed by using the following spin Hamiltonian:

$$\hat{H} = -2J\hat{S}_{Cu}\hat{S}_{Cu} - 2j(\hat{S}_{Cr}\hat{S}_{Cu} + \hat{S}_{Cr}\hat{S}_{Cu}) + D(\hat{S}_z^2)_{Cr} + \sum_i g_i\mu_B\hat{S}_i H, \quad (1)$$

where J is the copper–copper exchange coupling parameter and j is the chromium–copper exchange coupling parameter. In a first approach, the magnetic interaction between chromium(III) and copper(II) centres was neglected ($j = 0$). In fact, several reports on chromium(III)–copper(II) dimers showed that this interaction is zero or weakly antiferromagnetic [22]. In this case, the magnetic behaviour of the compound is approximated by the sum of the contributions of a copper(II) dimer (Bleaney–Bowers equation) [23] and two isolated chromium(III) ions. This corresponds to the following analytical expression for the $\chi_M T$ product:

$$\chi_M T = \chi_{B\text{–}B}T + 2\chi_{Cr}T,$$
$$\chi_{B\text{–}B}T = \frac{g_{Cu}^2}{4}\cdot\frac{3\exp(2J/T)}{3\exp(2J/T)+1},$$
$$\chi_{Cr}T = \frac{g_x^2}{4}\cdot\frac{1+(3T/4D)[1-\exp(-2D/T)]}{1+\exp(-2D/T)} + \frac{g_z^2}{32}\cdot\frac{1+9\exp(-2D/T)}{1+\exp(-2D/T)}, \quad (2)$$

where D is the zero-field splitting parameter of the Cr^{3+} ion. Least-squares fit (Fig. 4, dashed line) of $\chi_M T$ for **1** through Eq. (2) affords the following set of parameters: $J = -5\ cm^{-1}$, $|D| = 9.3\ cm^{-1}$ (the g values were fixed to $g = 2.0$). However, the correlation factor for this fit is low ($R = 0.994$) and the D value obtained is abnormally high, as compared to those observed in similar systems [12–18]. The introduction of an intermolecular interaction term (mean-field approximation, Eq. (3)) does not improve the quality of the fit, giving even higher values of D

$$(\chi_M T)_{inter} = \chi_M T\cdot\frac{T}{T-\frac{zj'\cdot\chi_M T}{Ng^2\mu_B^2}}. \quad (3)$$

This clearly indicates that the magnetic model described by Eq. (2) is not appropriate. This fact is corroborated by the analysis of the field dependence of the magnetisation of the tetramer. Clearly, the calculated data using the above-mentioned parameters (dashed line in Fig. 5) deviate considerably downwards from the experimental points at high field values. In a second step, the magnetic data (thermal variation of $\chi_M T$ and field dependence of the magnetisation) were simultaneously analysed through the full spin Hamiltonian (1) [24]. A set of valuable parameters for the fit of both experimental curves was found for positive values of J and D. These two parameters were strongly correlated and D was allowed to vary in the range $|D| < 5\ cm^{-1}$. In all cases, the fitting procedure gave negative values of j and the best-fit data (Fig. 4, solid line) afforded the following set of parameters: $J = +2\ cm^{-1}$, $j = -0.65\ cm^{-1}$, $|D| = 4.5\ cm^{-1}$. A mean value for the g factor $(g_{Cu} + g_{Cr})/2$ was used, with $g_{Cr} = 1.98$ and $g_{Cu} = 2.167$, as obtained from the EPR spectrum (vide infra). A scaling factor $C = 0.93$ was also introduced to account for possible impurities. The D value is still high as compared with the literature data and should be regarded as an upper limiting value that takes also into account the intermolecular interactions. Moreover, these parameters give a reasonably good fit of the isothermal magnetisation performed at 2 K (solid line in Fig. 5).

The ferromagnetic nature of the weak interaction in the central dicopper unit is not surprising, as the magnetic properties of oxalato-bridged dinuclear copper(II) complexes have been analysed in detail [25]. Strong antiferromagnetic interactions are expected when the $d_{x^2-y^2}$ metal orbitals lie in the plane [26,27] of the oxalato bridging group, whereas weak ferromagnetic interactions are observed in a few cases where the two metal orbitals lie in parallel planes that are perpendicular to the oxalato bridge (the so-called parallel arrangement) [28,29]. This particular requirement is satisfied in the structure of **1** (Fig. 6). The two copper(II) cations are related by an inversion centre located in the middle of the oxalato bridging ligand, in such a way that their corresponding N_2O_2 basal planes are strictly parallel. This geometry is very similar to that previously observed in the homometallic chain $[Cu(bpy)(ox)]\cdot 2H_2O$, where a

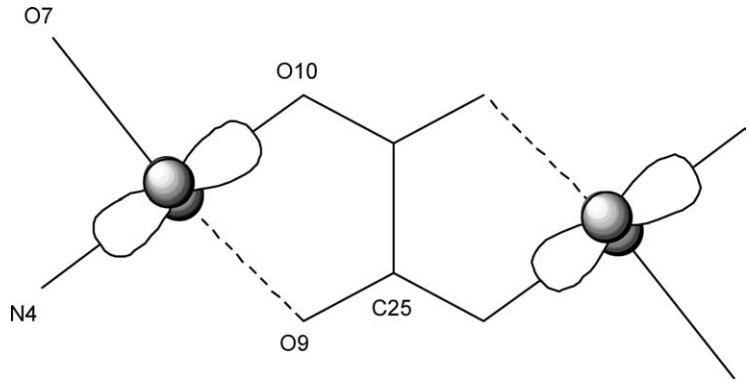

Fig. 6. Orbital diagram showing the coparallel arrangement of the copper(II) $d_{x^2-y^2}$ orbitals.

ferromagnetic interaction ($J = +1.22$ cm^{-1}) was also observed [30]. The higher value of the interaction parameter ($J = +2$ cm^{-1}) observed in our case may be attributed to a smaller axial distance (Cu(1)–O(9): 2.242(5) Å versus 2.313(2) Å in $[Cu(bpy)(ox)] \cdot 2H_2O$).

The exchange coupling between adjacent octahedral chromium(III) and copper(II) ions through an oxalate anion in dimeric species has been reported to be weakly ferromagnetic [31]. The observed behaviour was explained in terms of strict orthogonality between t_{2g} and e_g magnetic orbitals of the chromium(III) and copper (II) centres, respectively. This argument is valid for an ideal coplanar arrangement of the axially distorted copper(II) basal plane and the plane of the bridging ligand. In other cases, as in compound **1**, the arrangement of these planes is perpendicular and the elongated axis of the copper(II) ion is extremely bent (O(7)–Cu–O(9) = 159.9°). Under these circumstances, the copper magnetic orbital can have some d_{z^2} character and it can overlap with the chromium(III) orbitals of the same symmetry, stabilising an antiferromagnetic interaction.

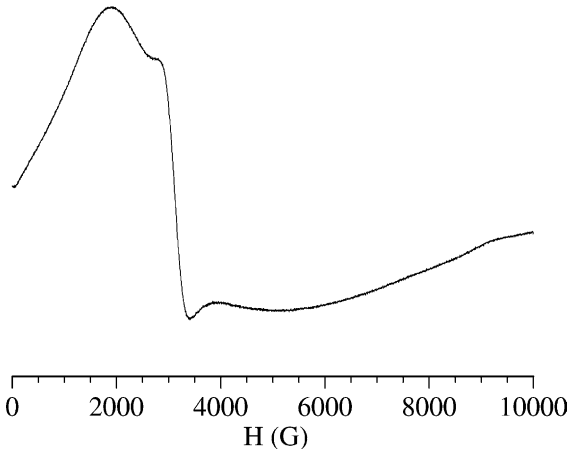

Fig. 7. EPR spectrum of **1** at room temperature.

3.3. EPR spectra

The EPR spectrum of **1** at room temperature (Fig. 7) shows a broad feature centred at $g = 2.167$ that can be attributed to the copper(II) centres. The shape of this EPR band does not change significantly with temperature and the position of the g-factor remains also unaltered down to 4 K (see Supplementary Material).

4. Conclusion

In this paper we have described the synthesis, structure and magnetic properties of the tetranuclear compound $[Cr_2Cu_2(bpy)_4(ox)_5] \cdot 2H_2O$ (**1**). Although the magnetic properties of dinuclear and extended oxalato-bridged compounds are known in detail, reports on oligonuclear species are rather scarce. The analysis of the structure and magnetism of the title compound has been compared to previous work on dinuclear copper(II) and chromium(III)–copper(II) complexes. Complex **1** belongs to a rare class of dicopper(II) μ-oxalato-compounds that exhibit a parallel arrangement of the magnetic orbitals in a plane perpendicular to the oxalate bridge. This arrangement hinders the appearance of strong exchange coupling between the adjacent metal centres, but stabilises a positive (ferromagnetic) interaction within the central dicopper subunit.

5. Supplementary material

Figure S1 showing the EPR spectra of **1** in the 300–4.2 K range is available from the authors on request. Crystallographic data for the structure analysis have been deposited with the Cambridge Crystallographic Data Center, CCDC No. 203684 for **1**. Copies of this information may be obtained free of charge from CCDC, 12 Union Road, Cambridge, CB2 1EZ, UK (fax: +44-1223-336033; e-mail: deposit@ccdc.cam.acuk or www: http://www.ccdc.cam.ac.uk).

Acknowledgements

Dr. Giménez-Saiz and Mr. Martínez-Agudo are acknowledged for their continuous support in the magnetic and X-ray measurements. We also thank financial support from Projects No. HPRN-CT-1999-00012 (EU), MAT2001-5408-E (MCYT) and Programa "Ramón y Cajal" (MCYT). M.C.G. thanks the Generalitat Valenciana for a Ph.D. fellowship.

References

[1] H. Tamaki, Z.J. Zhong, N. Matsumoto, S. Kida, M. Koikawa, N. Achiwa, Y. Hashimoto, H. Okawa, J. Am. Chem. Soc. 114 (1992) 6974.
[2] S. Decurtins, H.W. Schmalle, P. Schneuwly, H.R. Oswald, Inorg. Chem. 32 (1993) 1888.
[3] S. Decurtins, H.W. Schmalle, H.R. Oswald, A. Linden, J. Ensling, P. Gütlich, A. Hauser, Inorg. Chim. Acta 216 (1994) 65.
[4] S. Decurtins, H.W. Schmalle, R. Pellaux, New J. Chem. 22 (1998) 117.
[5] S.G. Carling, C. Mathonière, P. Day, K.M.A. Malik, S.J. Coles, M.B. Hursthouse, J. Chem. Soc. Dalton Trans. (1996) 1839.
[6] R. Pellaux, H.W. Schmalle, R. Huber, P. Fischer, T. Hauss, B. Ouladdiaf, S. Decurtins, Inorg. Chem. 36 (1997) 2301.
[7] S. Decurtins, H.W. Schmalle, P. Schneuwly, J. Ensling, P. Gütlich, J. Am. Chem. Soc. 116 (1994) 9521.
[8] S. Decurtins, H.W. Schmalle, R. Pellaux, R. Huber, P. Fischer, B. Ouladdiaf, Adv. Mater. 8 (1996) 647.
[9] E. Coronado, J.R. Galán-Mascarós, C.J. Gómez-García, V. Laukhin, Nature 408 (2000) 447.
[10] M.E. Von Arx, A. Hauser, H. Riesen, R. Pellaux, S. Decurtins, Phys. Rev. B 54 (1996) 15800.
[11] E. Coronado, J.R. Galán-Mascarós, C.J. Gómez-García, J.M. Martínez-Agudo, Inorg. Chem. 40 (2001) 113.
[12] M.C. Muñoz, M. Julve, F. Lloret, J. Faus, M. Andruh, J. Chem. Soc. Dalton Trans. (1998) 3125.
[13] G. Marinescu, R. Lescouëzec, D. Armentano, G. De Munno, M. Andruh, S. Uriel, R. Llusar, F. Lloret, M. Julve, Inorg. Chim. Acta 336 (2002) 46.
[14] G. Marinescu, M. Andruh, R. Lescouëzec, M.C. Muñoz, J. Cano, F. Lloret, M. Julve, New J. Chem. 24 (2000) 527.
[15] J.A. Broomhead, Aust. J. Chem. 15 (1962) 228.
[16] F.D. Rochon, R. Melanson, M. Andruh, Inorg. Chem. 35 (1996) 6086.
[17] M. Andruh, R. Melanson, C.V. Stager, F.D. Rochon, Inorg. Chim. Acta (1996) 309.
[18] N. Stanica, C.V. Stager, M. Cimpoesu, M. Andruh, Polyhedron 17 (1998) 1787.
[19] A. Altomare, M. C Burla, M. Camalli, G.L. Cascarano, C. Giacovazzo, A. Guagliardi, A.G.G. Moliterno, G. Polidoro, R. Spagna, SIR97. A Program for the Automatic Solution and Refinement of Crystal Structures, University of Bari, Italy, 1996.
[20] G.M. Sheldrick, SHELXL97, Universität Göttingen, Germany, 1997.
[21] M. Nardelli, J. Appl. Cryst. 32 (1999) 563.
[22] R, Lescouëzec, G. Marinescu, J. Vaissermann, F. Lloret, J. Faus, M. Andruh, M. Julve, Inorg. Chim. Acta (2003) in press.
[23] B. Bleaney, K.D. Bowers, Proc. R. Soc. London A (1952) 214.
[24] J.J. Borrás-Almenar, J.M. Clemente-Juan, E. Coronado, B.S. Tsukerblat, J. Comput. Chem. 22 (2001) 985.
[25] O. Kahn, Angew. Chem. Int. Ed. Engl. 24 (1985) 834, and references therein.
[26] M. Julve, J. Faus, M. Verdaguer, A. Gleizes, J. Am. Chem. Soc. 106 (1984) 8306.
[27] O. Castillo, I. Muga, A. Luque, J.M. Gutiérrez-Zorilla, J. Sertucha, P. Vitoria, P. Román, Polyhedron 18 (1999) 1235.
[28] M.L. Calatayud, I. Castro, J. Sletten, F. Lloret, M. Julve, Inorg. Chim. Acta 300–302 (2000) 846.
[29] O. Costisor, M. Brezeanu, Y. Journaux, K. Mereiter, P. Weinberger, W. Linert, Eur. J. Inorg. Chem. (2001) 2061.
[30] H. Oshio, U. Nagashima, Inorg. Chem. 31 (1992) 3295.
[31] M. Ohba, H. Tamaki, N. Matsumoto, H. Okawa, Inorg. Chem. 32 (1993) 5385.